Journal of Power Sources 238 (2013) 388–394

Contents lists available at SciVerse ScienceDirect

Journal of Power Sources

journal homepage: www.elsevier.com/locate/jpowsour

On the cycling stability of lithium-ion capacitors containing soft carbon as anodic material

M. Schroeder, M. Winter, S. Passerini, A. Balducci*

Westfälische Wilhelms Universität, Institut für Physikalische Chemie-MEET, Corrensstr. 28/30, 48149 Münster, Germany

HIGHLIGHTS

- Soft carbons can be successfully used for the realization of high performance LICs.
- LIC containing soft carbon display high power and energy.
- LIC containing display stable performance for 50,000 cycles.

ARTICLE INFO

Article history:
Received 9 January 2013
Received in revised form
6 March 2013
Accepted 10 April 2013
Available online 19 April 2013

Keywords:
Lithium-ion capacitor
Soft carbon
Activated carbon
Petroleum coke

ABSTRACT

Petroleum coke (PeC), a soft carbon, displays excellent performance at high current densities so that it can be considered as a very promising material for high performance lithium-ion capacitors (LICs). PeC-based LICs deliver a specific energy and power of 48 Wh kg^{-1} and 9 kW kg^{-1}, respectively, upon charge–discharge tests carried out using a current density of 4.5 A g^{-1} (corresponding to 30 C). These values are outperforming those displayed by supercapacitors and lithium-ion batteries under the same condition, and such performance can be maintained for 50,000 cycles.

1. Introduction

Lithium-ion capacitors (LICs) are hybrid devices containing a lithium-ion battery (LIB) electrode combined with a supercapacitor (SC) electrode [1–3]. This electrode combination might lead to a device able to display a higher power output compared to LIBs, a higher energy output compared to SCs, and a cycling stability in between these two systems [4]. Although many combinations are possible, the use of a carbonaceous LIB anode together with an activated carbon (AC) positive electrode appears till now the most convenient [4–14]. As a matter of fact, such an electrode combination allows devices with a high cell voltage (up to 5 V), high energy and high power [8]. Two processes are simultaneously taking place during the charge–discharge of LICs: lithium insertion–extraction within the bulk of the carbonaceous anode and formation-depletion of a double layer on the AC positive electrode.

Graphite is the state-of-the-art anode in LIBs, it offers a Li insertion/extraction potential between 0.1 and 0.2 V vs. Li/Li^+, and so far has been the most used carbonaceous material for LICs (LICs containing graphite-based anode have been already commercialized) [4,8,10,13,15–17]. The results of these works showed that graphite can be successfully used in LICs, but due to diffusion limitations during charge, its use might limit the performance of these devices during cycling at high current densities [18]. Taking this point into account, the introduction of a material able to guarantee the same insertion potential as graphite, but with improved performance at high current densities could be therefore beneficial for high performance LICs.

Recently, we proposed the use of a soft carbon, petroleum coke (PeC), as anode for LICs [12]. PeC displays higher performance at high current densities compared to graphite, and it can be therefore considered as a very promising material for high performance LICs [13]. Nevertheless, many characteristics of PeC-based LICs still need to be further investigated. One of them is the cycling stability during test carried out at high current densities. Since a long term cycling stability is essential for LICs, this investigation appears

* Corresponding author.
E-mail address: andrea.balducci@uni-muenster.de (A. Balducci).

0378-7753/$ – see front matter © 2013 Elsevier B.V. All rights reserved.
http://dx.doi.org/10.1016/j.jpowsour.2013.04.045

Table 1
Dry composition and mass loading of all electrodes used in the present study.

	Electrode composition/%			Mass loading/mg cm^{-2}
	Active material	Conductive agent	Binder	
LICs				
PeC	90	5	5	1.9
AC	80	15	5	2.9
SCs				
AC	80	15	5	2.9
LIBs				
Graphite	87	5	8	1.4
$LiCoO_2$	87	8	5	3.4

Table 2
Current density (I) applied during the charge–discharge tests carried out on the LICs.

C-rate	$I_{\text{based on PeC}}$ A g^{-1}	$I_{\text{based on total mass}}$ A g^{-1}	I mA cm^{-2}
1	0.372	0.15	0.66
5	1.9	0.74	3.3
15	5.6	2.2	9.9
30	11.2	4.5	19.8
60	22.3	8.9	39.5

of importance to evaluate the advantages related to the use of PeC in LICs.

In this manuscript we investigate the cycling stability as well as the performance of LICs containing PeC as anodic material and a solution of 1 M $LiPF_6$ in Ethylene Carbonate–Dimethyl Carbonate (EC–DMC, 1:1, *w*:*w*) as electrolyte. This electrolyte is not as safe as the Propylene Carbonate (PC) we used in our previous study, but it offers two advantages compared to PC-based electrolyte. Firstly, it possesses a higher ionic conductivity (11 mS cm^{-1} at 25 °C), which is beneficial for high current cycling and secondly, due to the presence of EC, it also displays a better SEI (solid electrolyte interphase) forming ability on carbon [19]. Initially, the capacity and the cycling stability of the PeC-based LICs are evaluated using current densities close to that typical of SC (ranging from 0.7 A g^{-1} to 8.9 A g^{-1}). Afterwards, a detailed investigation about the electrodes behavior during these prolonged cycling is presented and the energy and the power of the investigated LICs are determined and compared with those of SCs and LIBs. Finally, the maximum operative voltage applicable for the considered LICs is evaluated.

2. Experimental

Petroleum coke PC-40OC (PeC, Timcal, Switzerland, specific BET surface area: 3.98 m^2 g^{-1}, D90 40 μm) and activated carbon DLC Super 30 (AC, Norit, USA, specific BET surface area 1400 m^2 g^{-1}) were used as active materials (AMs), sodium carboxymethylcellulose (CMC) (Walocel CRT 2000 PA, Dow Wolff Cellulosics, Germany) as binder and Super C65 (Timcal, Switzerland) as conducting agent.

All electrodes used in this work were prepared using the procedure described in literature [12]. The dry compositions of the electrodes used in this work are listed in Table 1.

All electrochemical tests were carried out using 3-electrode Swagelok®-type cells (electrode area 1.13 cm^2). To avoid contamination by oxygen or humidity the cells were assembled in an Argon filled glovebox (MBraun, the H_2O and O_2 content was below 0.1 ppm). The reference electrode consisted of metallic Lithium (Chemetall, Germany). The used electrolyte was LP30 (1 M $LiPF_6$, EC:DMC 1:1, SelectiLyte, Merck). One layer of Whatman GF/D glass microfiber filter (thickness 675 μm) was used as separator and it was soaked with 140 μL of electrolyte.

The electrochemical tests were carried out in climatic chambers at 20 °C with a MACCOR Battery tester 4300 (Maccor Inc., USA) and a VMP multichannel potentiostatic–galvanostatic system (VMP, Biologic Science Instrument, France). All potentials quoted in this manuscript refer to the Li/Li$^+$ potential. The theoretical capacity of graphite (372 mAh g^{-1}, based on the mass of the anode, corresponding to 149 mAh g^{-1} based on both electrode masses) was used for the definition of the C-rate applied in all tests. The used currents are listed in Table 2.

Cyclic voltammetries on the PeC and AC-based electrodes were carried out at scan-rates ranging from 100 μV s^{-1} to 200 mV s^{-1}. Before starting the charge–discharge tests of the LICs, the PeC anode was charged/discharged four times at a rate of C/20 and charged one time at C/40 with the metallic Li reference electrode as counter electrode in a two electrode setup. The AC positive electrode was charged at C/40 to a cut-off potential of 4.2 V the same

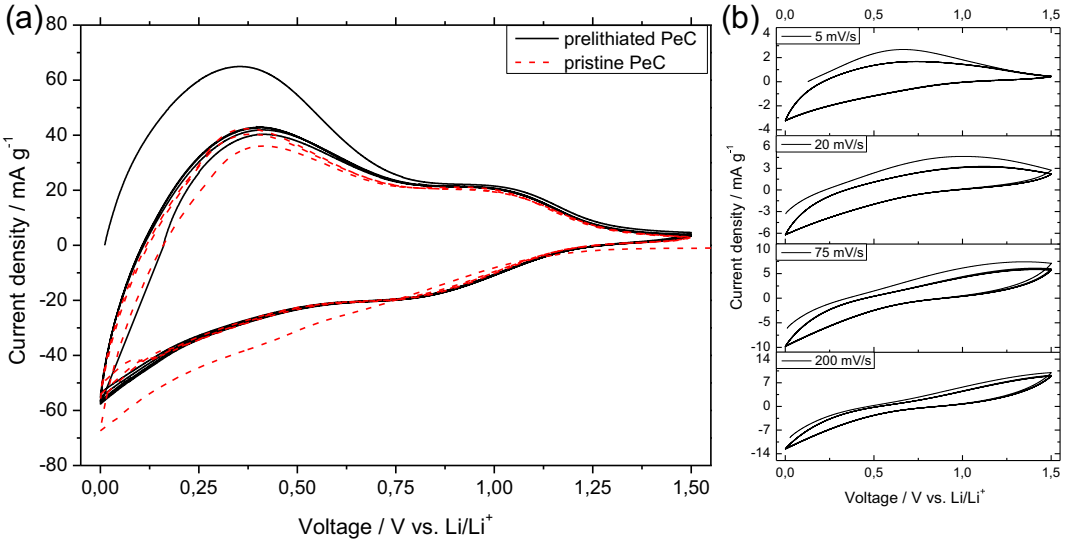

Fig. 1. (a) CVs of two PeC-based electrodes (pristine and pre-lithiated) obtained using a scan rate of 100 μV s^{-1}; (b) CVs of the pre-lithiated PeC-based electrode during test carried out using scan rate ranging from 5 to 200 mV s^{-1}.

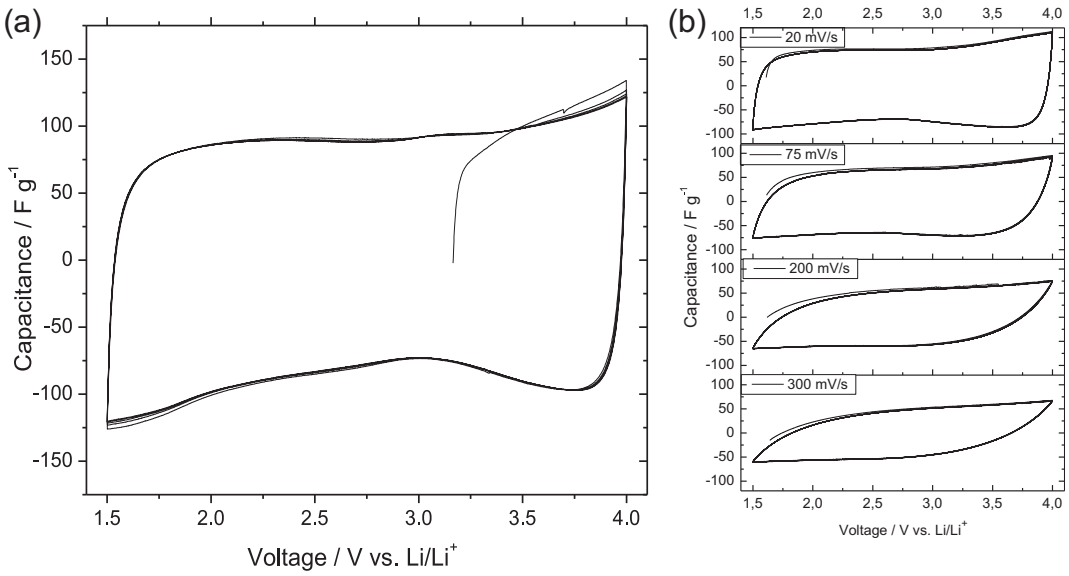

Fig. 2. (a) CV of an AC-based electrodes obtained using a scan rate of 5 mV s^{-1}; (b) CVs of the same electrode during test carried out using scan rate ranging from 20 to 300 mV s^{-1}.

way [12]. After this initial pre-charging, no further lithiation by the Li reference electrode was done. The LICs were cycled using cut-off voltages of 0.0 and 4.0 V. A discharge cut-off potential of 1.5 V was applied for the AC cathode to prevent irreversible Li insertion. Neither constant voltage charging/discharging steps nor resting steps were applied during cycling.

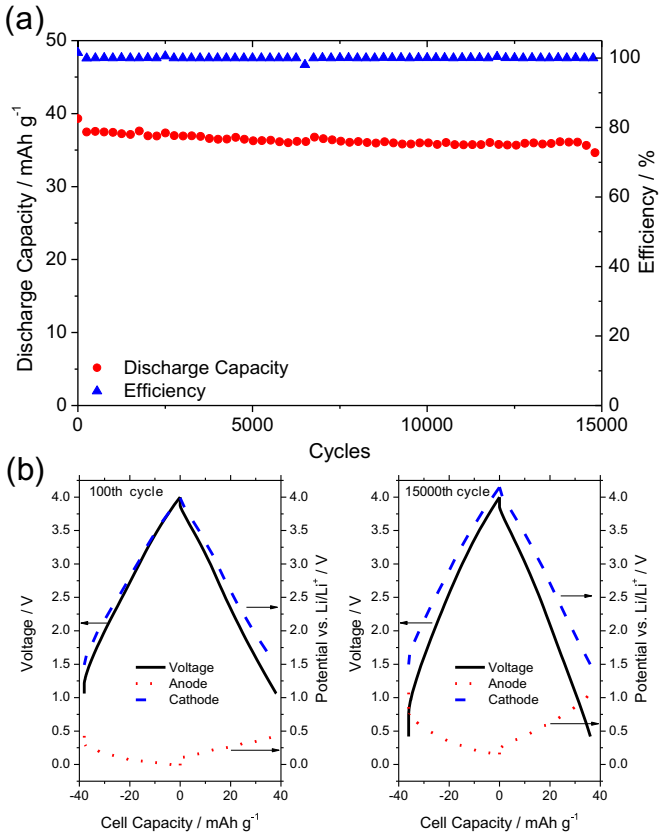

Fig. 3. (a) Long-term performance of a LIC operating in the range between 0 and 4 V during continuous charge–discharge cycles performed at the current density of 0.74 A g^{-1} (corresponding to 5 C). (b) Comparison of the voltage profiles at the beginning and at the end of the cycling for the same LIC.

The specific capacity of the LICs was calculated on the basis of the total electrode active material mass (PeC and AC). The average energy and power of the LICs as well as of the other devices considered for comparison were calculated as indicated in the reference [20]. The SCs used for comparison consisted of two AC-based electrodes, and 1 M Et_4NBF_4 in PC was used as electrolyte. The LIBs used for comparison consisted of a $LiCoO_2$-based cathode, a graphite-based anode and 1 M $LiPF_6$ in EC:DMC 1:1 as electrolyte [21]. The composition of these electrodes can also be found in Table 1. Both reference cells were lab-made [12].

3. Results and discussion

Fig. 1a shows the cyclic voltammetry (scan-rate 100 μV s^{-1}) of two PeC-based anodes between 0.0 and 1.5 V. The two anodes displayed different state of charge: one electrode was pre-lithiated using a protocol similar to that of reference [12], while the second one was used as prepared (pristine). As shown, except during the first cycle both voltammograms early superpose completely, indicating that the pre-lithiation did not affect the electrode capacity. From the figure it is visible that in the electrodes the insertion takes place mostly between 200 and 0 mV, while the Li extraction peak is around 350 mV. A second Li insertion/extraction signal can be found around 800 mV. Fig. 1b shows the CVs of a pre-lithiated PeC anode performed at different scan-rates (from 5 to 200 mV s^{-1}) between 0.0 and 1.5 V. Considering the figure, it appears evident that the increase of the scan-rates results in a shift of the charge potential to lower and of the discharge potential to higher values, respectively. In contrast to Fig. 1a only one charging step can be seen for the electrode, and the second discharging step could be only perceived using scan-rates of 5 mV s^{-1}. When high scan-rates are applied a reversible insertion–extraction of lithium seems to take place only in the region potential around 800 mV.

Fig. 2 shows the evolution of the specific capacitance of an AC-based electrode in the potential range between 1.5 and 4 V. As shown, in this potential range the AC electrode displays, as expected, the typical rectangular shape due to the formation of a double layer between the electrode surface and the electrolyte. Under this condition the electrode displayed a specific capacitance of 80 F g^{-1}. When the scan rate was increased (see Fig. 2b) the shape

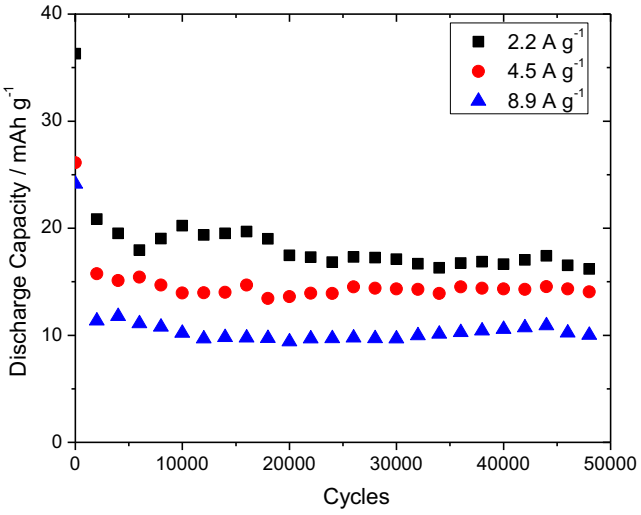

Fig. 4. Evolution of the capacity (referred to the total active mass) over 50,000 cycles of LICs operating in the range between 0 and 4 V during continuous charge–discharge cycles performed at the current densities of 2.2 A g^{-1}, 4.5 A g^{-1}, and 8.9 A g^{-1} (corresponding to 15 C, 30 C and 60 C, respectively).

of the CV became less ideal due to the increased resistance. Nevertheless, no faradaic reactions were observed.

Fig. 3 shows the cycling performance of a LIC containing a PeC-based anode and an AC-based cathode during charge–discharge tests carried out with a current density of 0.74 A g^{-1} (based on both electrode masses, corresponding to 5 C). As shown in the figure, the LIC displayed an initial capacity of 39 mAh g^{-1} (referred to the total active material). After a slight decrease of around 5% during the first cycles, the device displayed a stable capacity of 37 mAh g^{-1} for the following 15,000 cycles (Fig. 3a). Fig. 3b shows the cell voltage as well as the individual electrode potentials of the considered LIC at the beginning and the end of cycling. As shown, the LIC and its electrodes worked in the desired voltage and potential windows. While the anode was cycled between 0.0 and 0.4 V, where most of the Li insertion/extraction takes place, the AC used a very wide window between 1.5 and 4 V so that a maximum of capacity can be achieved. During cycling a slight shift of the anode potential toward higher values occurred. At the end of cycling the anode potential moved between 0.15 and 1 V, a region of potential in which a sufficient amount of Li can still be inserted and extracted (see Fig. 1).

As mentioned above, a high cycle life at high current densities is essential for LICs. Taking this point into account, the cycling stability of the LIC was therefore considered. Fig. 4 shows the long-term performance displayed by the LICs during charge–discharge cycles carried out at current densities of 2.2 A g^{-1}, 4.5 A g^{-1}, and 8.9 A g^{-1} (corresponding to 15 C, 30 C and 60 C, respectively, considering the masses of both electrodes). As shown, also when these high current densities (typically used in SC) were applied, the LICs displayed excellent performance. When current densities of 2.2 A g^{-1} and 4.5 A g^{-1} were used, the LIC displayed capacity of ca. 20 mAh g^{-1} and 15 mAh g^{-1}, respectively. When a current density of 8.9 A g^{-1} was applied, the LICs displayed a capacity of about 10 mAh g^{-1}. Even though these values were lower than that observed in the previous test (40–50% of the capacity at

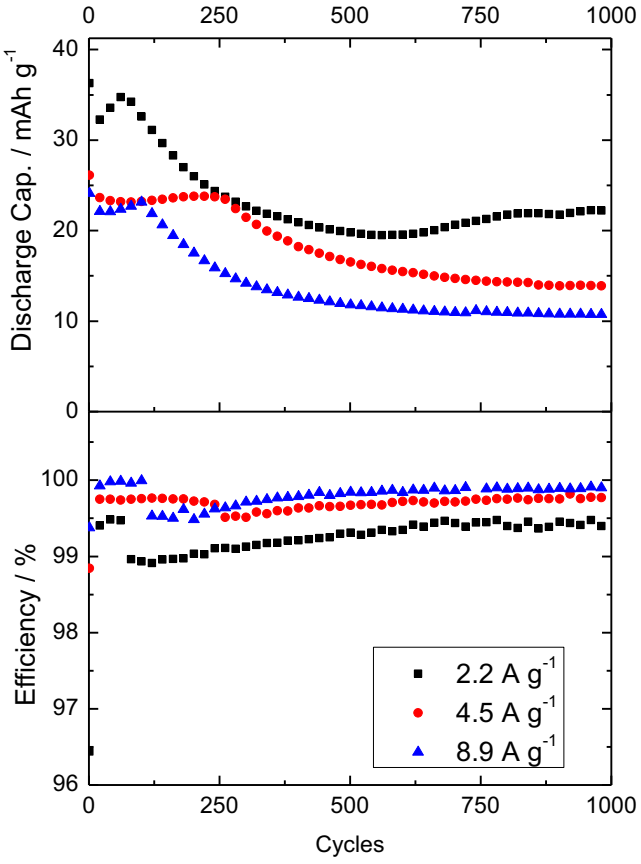

Fig. 5. Close-up of Fig. 4, which shows the evolution of the capacity (referred to the total active mass) and coulombic efficiency over the initial 1000 cycles of LICs operating in the range between 0 and 4 V during continuous charge–discharge cycles performed at the current densities of 2.2 A g^{-1}, 4.5 A g^{-1}, and 8.9 A g^{-1} (corresponding to 15 C, 30 C and 60 C, respectively).

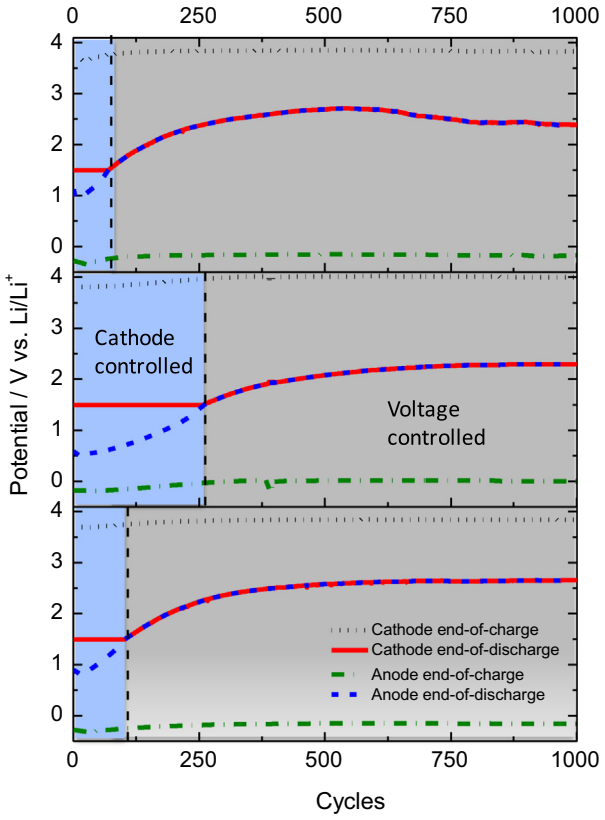

Fig. 6. Evolution of the end-of-charge and end-of-discharge of anode and cathode of LICs initial over the initial 1000 cycles of LICs operating in the range between 0 and 4 V during continuous charge–discharge cycles performed at the current densities of 2.2 A g^{-1}, 4.5 A g^{-1}, and 8.9 A g^{-1}.

0.74 mA g^{-1}) it is worth to taking into account that the applied current densities for this experiments were considerably higher. Moreover, it is important to note that the achieved capacity was fully maintained for 50,000 cycles at all considered current densities.

As shown in Fig. 4, all investigated LICs displayed an initial strong fading. Fig. 5 shows the evolution of the capacity (Fig. 5a) and of the coulombic efficiency (Fig. 5b) of the three LICs considered above during the first 1000 cycles of the charge–discharge test. All three LICs showed a rather similar behavior during these initial cycles. As a matter of fact, all of them showed a strong decrease of capacity in the first 30–50 cycles. During these cycles the efficiency of the charge–discharge was constantly increasing. After this fading, the capacity of the LICs started to increase again for a few hundred of cycles, and at the end of this period the LICs displayed a capacity similar to that they showed at the really beginning of cycling. The number of cycles necessary to come back to the initial values of capacity was different for each considered LICs and it did not appear related to the applied current density. During these cycles the efficiency of the charge–discharge process was rather constant and close to 100%. After this increase, a second capacity decrease was observed for all LICs. This fading was not so intense as the first one, but it occurred for a higher number of cycles compared to previous one. Interestingly, for all LICs the beginning of the second fading corresponded to a quite marked decrease of charge–discharge efficiency. During cycling the charge–discharge efficiency increased again, and at the end of the fading process was close to 100% for all LICs. At the end of this fading period, the LICs entered in a plateau of capacity, which was then maintained for 50,000 cycles (see Fig. 4). During these cycles the efficiency of the charge–discharge process was always close to 100% for all LICs.

Considering these results, PeC-based LICs seem therefore to across four different regions/states with different behavior of the efficiency, the capacity, its fading rate and the electrode potentials during their initial (1000) charge–discharge cycles. Such behavior can better be understood considering the potential values at the end-of-charge and end-of-discharge of the LICs electrodes. As shown in Fig. 6 during cycling the anode and the cathode of the LICs were subject to a dynamic change, and the potential reached by the electrodes at the end-of-discharge process changed considerably over cycling. As shown, during the first two regions mentioned above the discharge process of the LICs was limited by the cathodic cut-off potential of 1.5 V. Initially, the efficiency of the charge–discharge process was not optimal (see Fig. 5), but after some cycles the process become more effective and a sort of dynamic equilibrium was reached. During this time the anodic end-of-discharge potential increased over cycling. As a consequence, the voltage window also increased, leading to the increase of capacity observed above. After a certain number of cycles, because of the increase of the end-of-discharge potential of the anode, the anodic and the

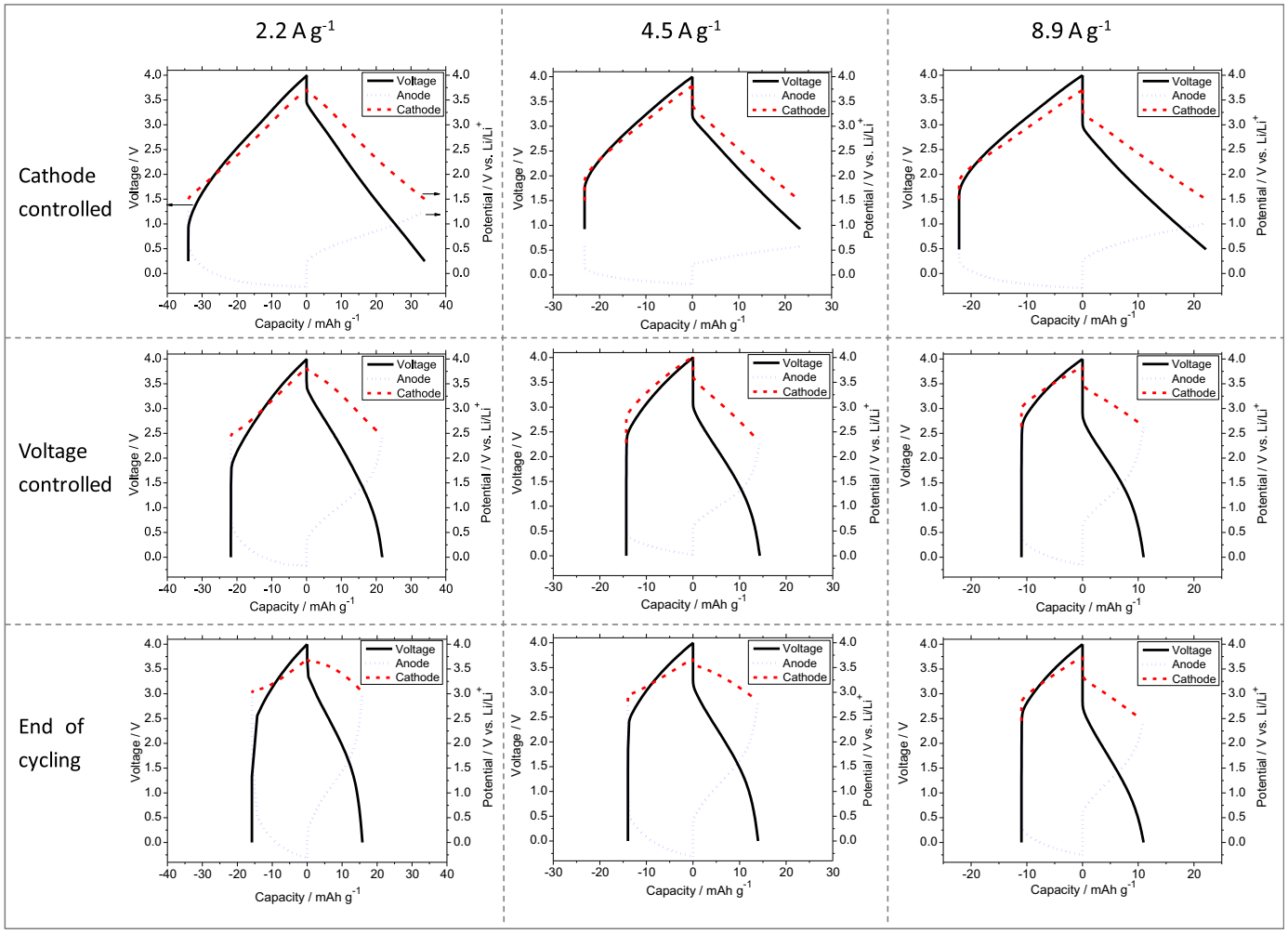

Fig. 7. Comparison of the anode and cathode potential as well as of the LICs voltage of LICs operating in the range between 0 and 4 V during continuous charge–discharge cycles performed at the current densities of 2.2 A g^{-1}, 4.5 A g^{-1}, and 8.9 A g^{-1}.

Table 3
Ohmic drop observed for the LICs the anode and the cathode during the charge–discharge tests.

$I_{based\ on\ total\ mass}$ A g^{-1}	LIC ohmic drop V	Anode ohmic drop V	Cathode ohmic drop V
0.74	0.15	0.11	0.04
2.2	0.27	0.24	0.03
4.5	0.94	0.56	0.38
8.9	1.08	0.75	0.33

cathodic cut-off potentials meet. Starting from this point the LICs were only voltage controlled, and this change generated the reduction of efficiency described above. Afterwards, the cell reached a new equilibrium, which is then maintained for 50,000 cycles.

The four regions mentioned above can be consequently reduced to two: the "cathode-control" region and the "voltage-control" region. Fig. 7 shows the voltage and potential profiles of the LICs during "cathode-control" region, the "voltage-control" region and at the end of cycling (50,000 cycles). As shown, in the "cathode-control" region both electrodes worked in their optimal potential region, and the maximum of capacity was reached. In the "voltage-control" region the electrode potential excursion of both electrodes changed. In this region the positive electrode worked in a narrow, while the anode in a broader potential range with respect the beginning of cycling. This potential shift caused a reduction of the capacity of positive electrode (which is linearly proportional to the potential excursion of the electrode), but did not cause an increase of the anode capacity. As a consequence, the LICs showed a decreased capacity with respect to the "cathode-control" region. Nevertheless, it is very important to note that once the "voltage-control" region was reached, the LICs behavior become extremely stable. As shown in the figure, the voltage profiles at the beginning of the "voltage-control" region were basically identical to that observed after 50,000 cycles. It is very interesting that the LICs displayed a similar behavior for all three currents densities applied during the experiments. Clearly, the LICs iR drop was higher when high current densities were applied (see Table 3). Nevertheless, for all applied current the iR drop was not dramatic and a promising capacity was always delivers by the LICs. The behavior showed by the anode during these experiments confirm the high performance at high current densities. Moreover, taking also into account the CV experiments, these tests seem to indicate that the lithium insertion–extraction process occurring around 800 mV is positively contributing to the performance at high current of soft carbons.

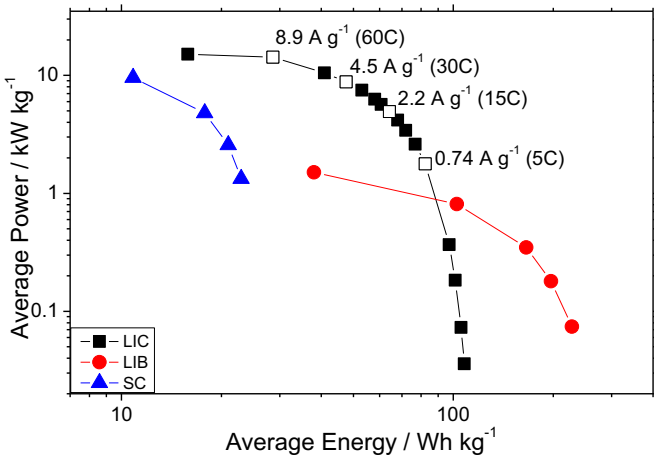

Fig. 8. Ragone plot for a LIC containing PeC electrode as anode. The average energy and power indicated to the figure referred to the total active mass of the LIC. For comparison, also the average energy and power (referred to the total active mass) of an electrochemical double-layer capacitor (SC) and a LIB are included in the figure.

Considering these results, it appears evident that LICs containing PeC as anodic material are certainly promising devices, able to display a very high and stable performance. This high performance is well visible also when the average energy and power of the investigated LIC are compared in a Ragone plot with those of a SC and of a LIB (Fig. 8). In order to avoid false results, the energy and power were calculated from charge–discharge tests carried out after the initial fading/conditioning of all devices. As shown in the figure, in the range of current densities investigated above, the considered LIC displays significantly higher power compared to LIBs, and significantly higher energy compared to SCs. For example, when a current density of 4.5 A g^{-1} was applied, the LIC displayed energy and power values of 48 Wh kg^{-1} and 9 kW kg^{-1}, respectively. These values are outperforming those of both SCs and LIBs and, as showed above, they can be fully maintained for thousands of cycles. To the best of our knowledge, these values of energy, power as well as cycling stability are among the highest so far reported for LICs [4,7,9–14,22]. Moreover, it is important to take into account that this very good performance (and cycling stability) has been obtained using current densities significantly higher than those applied for most of the LICs so far reported [4,7,9–14,22].

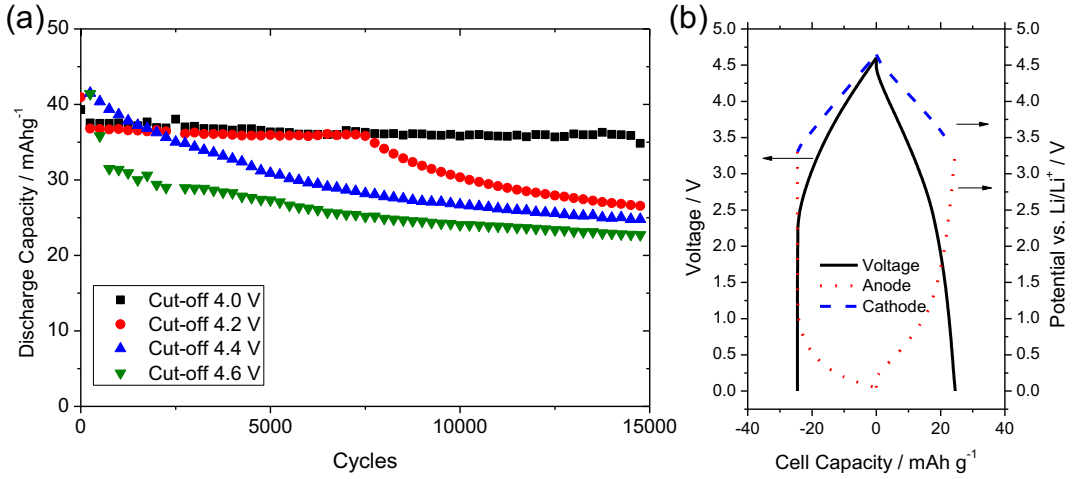

Fig. 9. (a) Long-term performance of a LIC operating in the range between 0 and different upper cut-off voltages (4.0 V, 4.2 V, 4.4 V and 4.6 V) during continuous charge–discharge cycles performed at the current density of 0.74 A g^{-1} (corresponding to 5 C). (b) Voltage profiles at the end of cycling for a LIC cycled up to 4.6 V.

The capacity, energy and power of the soft carbon-based LICs can be further increased using a higher cell voltage. Considering this point, we decided to investigate the performance of PeC-based LICs having cell voltages of 4.2 V, 4.4 V and 4.6 V. Fig. 9a shows the cycling behavior of these LICs as obtained during charge–discharge test carried out at 0.74 A g^{-1}. As expected, the initial capacity of these LICs was proportional to the cell voltage, and consequently the LIC operating at 4.6 V was the one able to display the highest initial capacity (43 mAh g^{-1}). Nevertheless, the higher the cell voltage was the stronger was the capacity fading during cycling. As shown in the figure, the LIC operating at 4.2 V displayed a stable behavior for about 7500 cycles but afterward its capacity constantly decreased. In the case of the LICs operating up to 4.4 V and 4.6 V, the capacity fading started immediately, and after 15,000 cycles both devices displayed a reduction of capacity of almost 50% with respect to their initial values. Fig. 9b shows as example the voltage and potential profiles of the LIC operating at 4.6 V after 15,000 cycles. At the end of cycling the positive electrode worked in a narrow, the anode in a broader potential range with respect to the first cycles, resulting in a reduced overall LIC capacity. As described above, such shift was also the responsible of the capacity reduction observed during the first cycles carried out at high current densities. Taking into account these results, the operative voltage of 4.0 V appears therefore as the maximum operative voltage can be applied for the realization of PeC-based LICs, containing 1 M $LiPF_6$ in EC:DMC (1:1) as electrolyte, able to display high cycling stability.

4. Conclusion

Soft carbons (e.g. PeC) are promising anodic materials for the realization of high performance LICs. They display high performance at high current densities and low self-discharge and these properties make their use in LICs particularly advantageous.

In this work we showed that PeC-based LICs display remarkable cycling stability during tests carried out using current densities close to that typical of SC (ranging from 0.7 A g^{-1} to 8.9 A g^{-1}). During the initial cycles of these LICs a conditioning process is occurring. This conditioning is mainly caused by a change of efficiency of the charge–discharge process, which in turn leads to a shift of electrode potential over cycling. However, as soon a dynamic equilibrium was reached, the behavior of PeC-based LICs became extremely stable. When the electrolyte 1 M $LiPF_6$ in EC:DMC (1:1) is used, the maximum operative voltage, that can be safely applied for PeC-based LICs is 4.0 V. As a matter of fact, when higher operative voltages are applied, the cycling stability of these LICs decreased dramatically. When a current density of 4.5 A g^{-1} is applied, a PeC-based LICs having a cell voltage of 4.0 V delivers energy and power of 48 Wh kg^{-1} and 9 kW kg^{-1}, respectively. This excellent performance can be maintained for 50,000 cycles. To the best of our knowledge, these values of energy, power as well as cycling stability are among the highest reported so far for LICs.

Acknowledgment

The authors wish to thank the Westfälische Wilhelms Universität Münster and the Ministerium für Innovation, Wissenschaft, Forschung und Technologie des Landes Nordrhein-Westfalen (MIWFT) and EVONIK (within the project EvoCarb) for the financial support. We gratefully appreciated the supply of materials by Norit Activated Carbon Holding (AC) and TIMCAL (PC-40OC and Super C65).

References

[1] J.P. Zheng, J. Electrochem. Soc. 150 (2003) A484.
[2] J.P. Zheng, J. Electrochem. Soc. 152 (2005) A1864.
[3] J.P. Zheng, J. Electrochem. Soc. 156 (2009) A500.
[4] J.-H. Kim, J.-S. Kim, Y.-G. Lim, J.-G. Lee, Y.-J. Kim, J. Power Sources 196 (2011) 10490.
[5] A. Yoshino, T. Tsubata, M. Shimoyamada, H. Satake, Y. Okano, S. Mori, S. Yata, J. Electrochem. Soc. 151 (2004) A2180.
[6] T. Aida, K. Yamada, M. Morita, Electrochem. Solid-State Lett. 9 (2006) A534.
[7] T. Aida, I. Murayama, K. Yamada, M. Morita, J. Electrochem. Soc. 154 (2007) A798.
[8] V. Khomenko, E. Raymundo-Piñero, F. Béguin, J. Power Sources 177 (2008) 643.
[9] D. Cericola, R. Kötz, Electrochim. Acta 72 (2012) 1.
[10] C. Decaux, G. Lota, E. Raymundo-Piñero, E. Frackowiak, F. Béguin, Electrochim. Acta 86 (2012) 282.
[11] K. Kuratani, M. Yao, H. Senoh, N. Takeichi, T. Sakai, T. Kiyobayashi, Electrochim. Acta 76 (2012) 320–325.
[12] M. Schroeder, M. Winter, S. Passerini, A. Balducci, J. Electrochem. Soc. 159 (2012) A1240.
[13] S.R. Sivakkumar, A.G. Pandolfo, Electrochim. Acta 65 (2012) 280.
[14] J. Ni, Y. Huang, L. Gao, J. Power Sources 223 (2013) 306.
[15] S.R. Sivakkumar, A.S. Milev, A.G. Pandolfo, Electrochim. Acta 56 (2011) 9700.
[16] JM Energy Corporation, http://www.jmenergy.co.jp/en/index.html, (last visited 22.02.13).
[17] S.R. Sivakkumar, J.Y. Nerkar, A.G. Pandolfo, Electrochim. Acta 55 (2010) 3330.
[18] M. Winter, K.-C. Moeller, J.O. Besenhard, in: G.-A. Nazri, G. Pistoia (Eds.), Lithium Batteries Science and Technology, Kluwer Academic Publisher, Boston, 2004.
[19] D. Guyomard, J.M. Tarascon, J. Electrochem. Soc. 140 (1993) 3071.
[20] A. Krause, P. Kossyrev, M. Oljaca, S. Passerini, M. Winter, A. Balducci, J. Power Sources 196 (2011) 8836.
[21] S. Krueger, R. Kloepsch, J. Li, S. Nowak, S. Passerini, M. Winter, J. Electrochem. Soc. 160 (2013) A542.
[22] W.J. Cao, J.P. Zheng, J. Power Sources 213 (2012) 180.